Cavity quantum electrodynamics with rare-earth ions in solids

Ding, D.

Citation

Ding, D. (2015, March 12). *Cavity quantum electrodynamics with rare-earth ions in solids*. *Casimir PhD Series*. Retrieved from https://hdl.handle.net/1887/32591

Author: Ding, Dapeng
Title: Cavity quantum electrodynamics with rare-earth ions in solids
Issue Date: 2015-03-12

Chapter 5

Yb-doped ring resonator at very low temperature

In Chapter 4 we studied the spontaneous emission (SE) rate of Yb^{3+} ions in a ring resonator from room temperature down to about 5 K. The observed Purcell enhancement of the SE rate increases with decreasing temperature due to a decreasing homogeneous linewidth of Yb^{3+}. We demonstrated a maximum Purcell factor of 3.6 at 5.5 K, which is, however, still limited by the homogeneous linewidth of Yb^{3+}. In order to fully benefit from our high-Q ring resonator, the homogeneous linewidth needs to be much smaller than the cavity linewidth and in such a limit the Purcell factor will be independent of the homogeneous linewidth.

In this chapter we investigate SE of Yb^{3+} ions in a ring resonator at very low temperature. According to the theory presented in Chapter 4, when the homogeneous linewidth of Yb^{3+} is reduced to be much smaller than the cavity linewidth at very low temperature, the 3D (cavity) Purcell factor is approximately proportional to Q_c/V independent of temperature with Q_c and V being the cavity quality factor and the mode volume, respectively. The thermally activated dipole depolarization that was studied in Chapter 4 is negligible within the lifetime of Yb^{3+} at very low temperature. Therefore only the TM_0 modes of the ring resonator are important for the Purcell effect since the ions are excited by the laser coupled to the TM_0 mode. Consequently, the maximum Purcell factor as given by Eq. (4.12) in Chapter 4 reads in a simple form:

$$F_\mathrm{m} = (F^1 + F^2 + F^3) f(y_0) \approx 8.96, \tag{5.1}$$

where the superscripts denote the dimension for each Purcell factor F^i, $f(y_0)$ is a spatial factor accounting for the Yb^{3+} sheet above the field maximum in the ring resonator, and both F and $f(y_0)$ are defined for the TM_0 mode.

5.1 Measurements and results

We study the Yb^{3+}-doped ring resonator as described in Chapter 4 using a closed-cycle dilution refrigerator. The refrigerator is operated by Arthur M. J. den Haan and Jelmer J. T. Wagenaar from the research group of professor Tjerk H. Oosterkamp, Leiden University. Figure 5.1 shows the refrigerator with its vacuum chamber opened and the sample mounted on the milli-Kelvin plate. Four optical fibers that are coupled to the ring resonator are routed out of the refrigerator via two fiber vacuum feedthroughs [58]. The setup used to measure the lifetime of Yb^{3+} is the same as that in Chapter 4 (see Fig. 4.4).

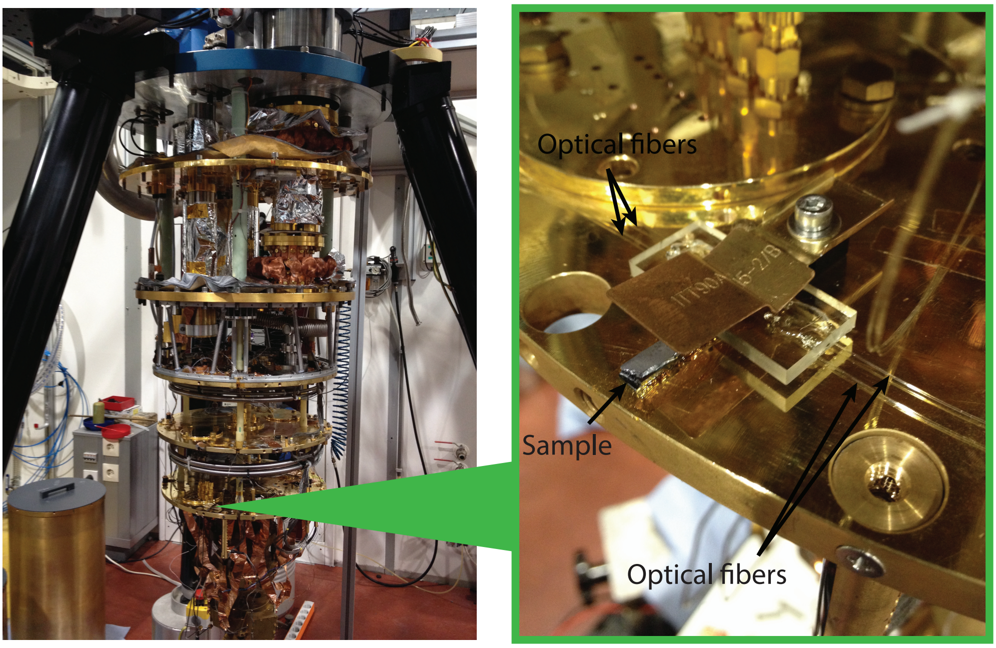

Figure 5.1: Photographs of the closed-cycle dilution refrigerator with its vacuum chamber opened (left) and the sample with Yb^{3+}-doped ring resonators mounted on the milli-Kelvin plate (right). Four optical fibers that are coupled to the ring resonator are routed out of the refrigerator via two fiber vacuum feedthroughs. The refrigerator is operated by Arthur M. J. den Haan and Jelmer J. T. Wagenaar from the research group of professor Tjerk H. Oosterkamp, Leiden University.

We carried out lifetime measurements in the temperature range of 12 mK–4.7 K using the same parameters as those presented in Chapter 4. A measured SE decay trace at 50 mK is shown in Fig. 5.2 in contrast to that measured at 5.7 K, which clearly demonstrates a larger decay rate at 50 mK. In order to extract the Purcell factor, we fit the data using the decay function described in Chapter 4 as shown in Fig. 5.2 assuming that the spatial distribution of Yb^{3+} in the cavity modes is the only source of inhomogeneity of the decay rate, and that collective effects among the ions can be neglected. The decay function follows the decay trace at initial times with higher decay rates but fails later ($t > 1$ ms) for the part with lower decay rates. The fit results in a free-space decay rate $k_0 = 2.00$ ms^{-1} and a maximum enhanced decay rate $k_\mathrm{m} = 11.7$ ms^{-1}. k_0 is too large compared with its value measured at 5.7 K (1.30 ms^{-1}) because the model apparently overestimates the decay rate at longer times (see also deviations between theory and experiment in Fig. 5.2).

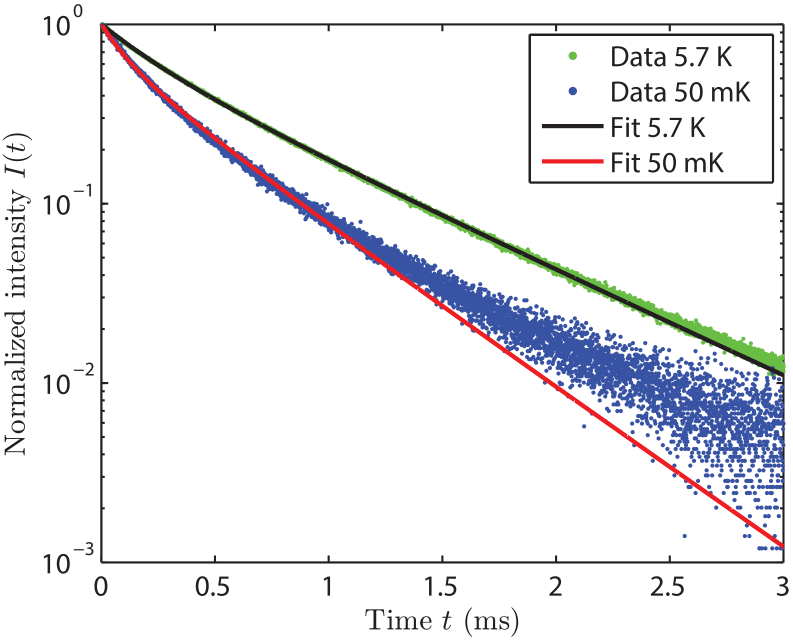

Figure 5.2: Measured spontaneous emission (SE) decay data at 5.7 K (green dots) and 50 mK (blue dots) in a logarithmic scale with time bins of 0.5 μs and the fits (black and red curves) to a decay function. The data are obtained by averaging over 5×10^5 single decay traces. The dark counts are subtracted and the maximum counts are normalized to unity. The absolute maximum counts of the data at 50 mK is lower than that at 5.7 K, because less ions spectrally overlap with the laser at 50 mK.

One of the possible reasons for the deviation of the model from the measured data is the collective effects among the ions that may become appreciable when the pure dephasing rate of Yb^{3+} is reduced significantly at very low temperature. This breaks the assumption of independent ions in the model. Another possible reason may be the different coupling efficiencies of the SE from the ions with different Purcell factors along the sheet of doping, which are assumed to be equal in the model. This assumption was proven to be a good approximation at high temperatures where both the 2D and 3D Purcell factors are small compared with the 1D Purcell factor. At very low temperatures the

3D Purcell factor is dominant for the ions close to the center of the mode and is much smaller for the ions at the edge of the mode, which results in a variation of the coupling efficiency for the ions along the sheet of doping with different values of k.

Nevertheless, because the decay function provides a reasonable fit to the part of the data with the fastest decay as shown in Fig. 5.2, we assume the extracted maximum enhanced decay rate $k_{\mathrm{m}} = 11.7\ \mathrm{ms}^{-1}$ from the fit is still reliable. This enables us to calculate the maximum Purcell factor F_{m} as $k_{\mathrm{m}}/k_{\mathrm{R}} = 9.0$ with $k_{\mathrm{R}} = 1.30\ \mathrm{ms}^{-1}$ being the radiative decay rate of Yb^{3+} that is extracted from the data measured at higher temperature in Chapter 4. This estimation yields good agreement with the theory and confirms that the fit of the decay function results in a reasonable extracted value of k_{m}.

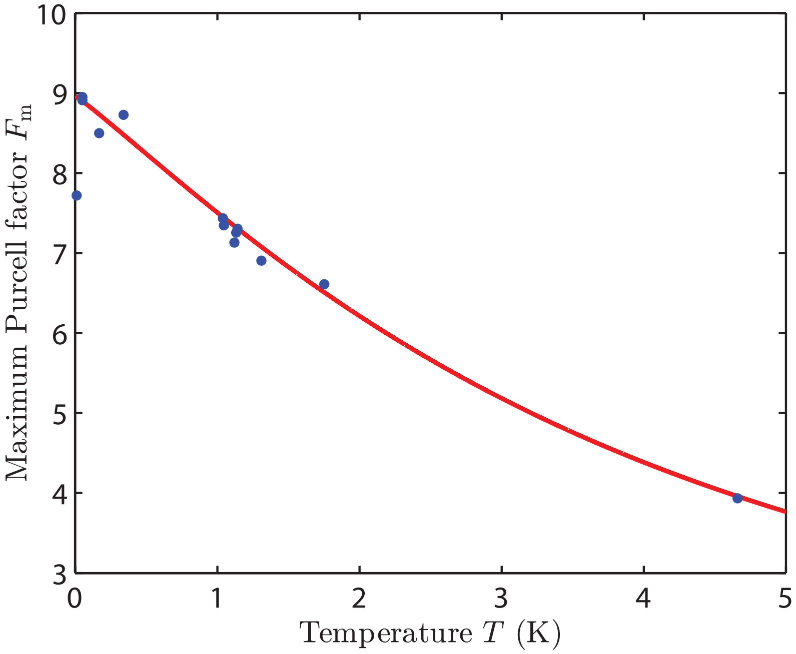

Figure 5.3: Measured maximum Purcell factor F_{m} (blue dots) as a function of temperature and the theoretical model (red curve) that includes the multi-dimensional Purcell effect and the dipole depolarization. The data are generally in good agreement with the theory except for $F_{\mathrm{m}} \approx 7.7$ at 12 mK which is apparently lower than the theory and also deviates from the trend of other data.

In the same way we obtain k_{m} from the fits to the decay traces at temperatures in the range of 12 mK–4.7 K and calculate $F_{\mathrm{m}} = k_{\mathrm{m}}/k_{\mathrm{R}}$. The values of F_{m} as a function of temperature and the theoretical curve that was obtained in Chapter 4 including the multi-dimensional Purcell effect and the dipole depolarization are shown in Fig. 5.3. The data are generally in good agreement with the theory, which verifies our theoretical model at lower temperatures compared with the temperature range in Chapter 4.

5.2 Discussions

$F_\mathrm{m} \approx 7.7$ at 12 mK is apparently lower than the theory and also deviates from the trend of other data. This can not be explained by the Purcell effect. At temperatures below about 100 mK, the pure dephasing rate of Yb^{3+} is much smaller than the cavity linewidth and the thermally activated dipole depolarization is negligible within the lifetime of Yb^{3+}. Therefore we would expect that the Purcell effect is independent of temperature. Neither can this be explained by the collective effects. The collective effects depend on the number of ions and the pure dephasing rate for the same coupling constant to the cavity. The pure dephasing rate of rare-earth ions in glass at very low temperature is worth more attention. In Chapter 4 we obtained a relation of the homogeneous linewidth (equal to the pure dephasing rate divided by π) of Yb^{3+} in pure silica with temperature as $5.0 \times T^{1.3}$ (MHz). This $T^{1.3}$ law has been proven to be still valid down to about 100 mK for a Nd^{3+}-doped pure silica fiber [76]. Below about 100 mK, the homogeneous linewidth deviates from the $T^{1.3}$ law [76] and tends to be independent of temperature [77], but it can be further reduced by applying a magnetic field for an Er^{3+}-doped silicate fiber [77]. We estimate the homogeneous linewidth of Yb^{3+} at 100 mK to be approximately 0.25 MHz (pure dephasing rate 0.79 MHz) by using our relation and assume this value to be constant for temperatures below 100 mK. With the same pure dephasing rate and excitation parameters in the experiment, the number of excited ions should be the same at temperatures below 100 mK. Therefore we would expect that the collective effects should be the same for the measurements at 12 mK and 50 mK. We will theoretically investigate the collective effects in Chapter 6.

In conclusion, we measured the SE rate of Yb^{3+} in a high-Q Si_3N_4 ring resonator in the temperature range of 12 mK–4.7 K. The maximum Purcell factor F_m that is extracted from the data is in good agreement with the theoretical model, which verifies our theoretical model at lower temperatures compared with the temperature range in Chapter 4. The value of F_m at 12 mK is apparently lower than the value that the theory predicts and also deviates from the trend of other data. This effect which can not be explained by the Purcell effect or by the collective effects has not been fully understood yet.